

RESEARCH ARTICLE

Evaluation of carotid plaque echogenicity based on the integral of the cumulative probability distribution using gray-scale ultrasound images

Xiaowei Huang^{1,2}, Yanling Zhang³, Long Meng¹, Derek Abbott⁴, Ming Qian¹, Kelvin K. L. Wong⁵, Rongqing Zheng³, Hairong Zheng¹, Lili Niu^{1*}

1 Paul C. Lauterbur Research Center for Biomedical Imaging, Institute of Biomedical and Health Engineering, Shenzhen Institutes of Advanced Technology, Chinese Academy of Sciences, Shenzhen, China, **2** Shenzhen College of Advanced Technology, University of Chinese Academy of Sciences, Shenzhen, China, **3** Department of Ultrasound, Third Affiliated Hospital, Sun Yat-sen University, Guangzhou, China, **4** Centre for Biomedical Engineering, and School of Electrical and Electronic Engineering, University of Adelaide, Adelaide, Australia, **5** School of Medicine, Western Sydney University, Campbelltown, New South Wales, NSW, Australia

* ll.niu@siat.ac.cn



OPEN ACCESS

Citation: Huang X, Zhang Y, Meng L, Abbott D, Qian M, Wong KKL, et al. (2017) Evaluation of carotid plaque echogenicity based on the integral of the cumulative probability distribution using gray-scale ultrasound images. PLoS ONE 12(10): e0185261. <https://doi.org/10.1371/journal.pone.0185261>

Editor: Yoshihiro Fukumoto, Kurume University School of Medicine, JAPAN

Received: January 17, 2017

Accepted: September 8, 2017

Published: October 4, 2017

Copyright: © 2017 Huang et al. This is an open access article distributed under the terms of the [Creative Commons Attribution License](https://creativecommons.org/licenses/by/4.0/), which permits unrestricted use, distribution, and reproduction in any medium, provided the original author and source are credited.

Data Availability Statement: All relevant data are within the paper and its Supporting Information files.

Funding: The work was supported by National Key R&D Program of China (2016YFC0104700), National Science Foundation Grants (NSFC Grant Nos. 11574341, 11674347, 81527901, 11325420, 11574342), Shenzhen Basic Science Research (JCYJ20160429190550139, JCYJ2016042918455 2717), and Natural Science Foundation of

Abstract

Objective

Carotid plaque echogenicity is associated with the risk of cardiovascular events. Gray-scale median (GSM) of the ultrasound image of carotid plaques has been widely used as an objective method for evaluation of plaque echogenicity in patients with atherosclerosis. We proposed a computer-aided method to evaluate plaque echogenicity and compared its efficiency with GSM.

Methods

One hundred and twenty-five carotid plaques (43 echo-rich, 35 intermediate, 47 echolucent) were collected from 72 patients in this study. The cumulative probability distribution curves were obtained based on statistics of the pixels in the gray-level images of plaques. The area under the cumulative probability distribution curve (AUCPDC) was calculated as its integral value to evaluate plaque echogenicity.

Results

The classification accuracy for three types of plaques is 78.4% (kappa value, $\kappa = 0.673$), when the AUCPDC is used for classifier training, whereas GSM is 64.8% ($\kappa = 0.460$). The receiver operating characteristic curves were produced to test the effectiveness of AUCPDC and GSM for the identification of echolucent plaques. The area under the curve (AUC) was 0.817 when AUCPDC was used for training the classifier, which is higher than that achieved using GSM (AUC = 0.746). Compared with GSM, the AUCPDC showed a borderline association with coronary heart disease (Spearman $r = 0.234$, $p = 0.050$).

Guangdong Province (2016TQ03X716, 2016TQ03R472). The funders had no role in study design, data collection and analysis, decision to publish, or preparation of the manuscript.

Competing interests: The authors have declared that no competing interests exist.

Conclusions

Our experimental results suggest that AUCPDC analysis is a promising method for evaluation of plaque echogenicity and predicting cardiovascular events in patients with plaques.

Introduction

Cardiovascular diseases significantly threaten human health and are the primary cause of death and disability worldwide [1]. Most myocardial infarctions, strokes, and acute coronary syndromes are caused by the rupture of unstable atherosclerotic plaques [2]. In recent years, growing evidence has been presented to support the association between plaque echogenicity and its vulnerability [3,4]. Echolucent plaques are dominated with lipid content, less calcification, less fibrous tissue, and tend to be more prone to rupture [5,6]. In addition, previous studies have demonstrated that plaque echolucency is associated with coronary events and future stroke [7,8]. Therefore, it is of significant interest to evaluate the plaque echogenicity, which may contribute to the identification of unstable plaques and for predicting cardiovascular events.

It is well-known that ultrasound imaging is a non-invasive technique for carotid atherosclerosis plaque examination. Ultrasound measurement of plaque echogenicity can provide a risk factor for predicting cardiovascular events [9–11]. Visual classification has been used to assess the plaque echogenicity in many previous studies [11–13], however, the results are operator-dependent. Recent studies have shown that computer assisted methods of plaque characterization using B-mode images can provide measurements in predicting clinical outcome [4,14–19]. Percentage white (PW) has been proposed as a metric for evaluation of echogenicity in carotid plaques, but it needs an intensity threshold to determine which pixels are echogenic (white) [14]. The process of PW feature extraction is relatively complex because the intensity threshold of each image is different. Texture analysis has been utilized to characterize carotid atherosclerotic plaques in symptomatic and asymptomatic patients [15–17], and it shows promise in the assessment of plaque echogenicity by combining the morphological characteristics of plaques [20]. However, the extraction of texture features requires high computational complexity. Recent studies have indicated that computerized measurement of the gray-scale median (GSM) is an objective and useful metric for assessment of the plaque echogenicity [4,18,19]. It is worthwhile noting that GSM is the fiftieth percentile of the probability distribution of gray-scale pixels, and it ignores the details of the probability distribution of plaques. Shankar et al. proposed a method to model the statistics of the pixels in the gray-level images of soft and hard plaques [21]. The cumulative probability distribution curves showed significant trends for these two types of plaques. Therefore, we suggest that the area under the cumulative probability distribution curve (AUCPDC) may be an effective parameter for evaluating plaque echogenicity.

The aim of this study is to examine whether the AUCPDC analysis is a useful method for the evaluation of plaque echogenicity and to further compare its efficiency with GSM.

Subjects and methods

A. Patients

The study protocol was approved by the Institutional Review Board of the third affiliated hospital of Sun Yat-sen University (Guangzhou, China). All participants provided written informed consent.

From September 2013 to March 2016, a total of 130 carotid plaques were collected from 74 volunteers, and 5 controversial plaques were excluded after visual classification by two sonographers. The remaining 125 carotid plaques (43 echo-rich, 35 intermediate and 47 echolucent plaques) from 72 volunteers were used in the following analysis.

B. Clinical and biochemical analyses

Blood samples were collected after an overnight fast for analysis of total cholesterol, triglyceride, high density lipoprotein cholesterol, low density lipoprotein cholesterol, apolipoprotein A1, apolipoprotein B100, fasting plasma glucose, and HbA_{1c}. The diagnostic criteria for hypertension was defined as systolic blood pressure ≥ 130 mmHg and/or diastolic blood pressure ≥ 80 mmHg or current use of antihypertensive agents. Diabetes was defined as fasting plasma glucose level of ≥ 7.0 mmol/L, and/or 2-hour plasma glucose value of ≥ 11.1 mmol/L, and/or HbA_{1c} level of $\geq 6.5\%$, and/or treatment with either hypoglycemic agents or insulin [22,23].

C. Images acquisition and preprocessing

Ultrasound images of carotid plaques were collected by a sonographer that has 5 years of experience in vascular imaging using an Aplio XG (SSA-790A) (Toshiba Medical Systems, Japan) equipped with a 5–12 MHz linear-array transducer (PLT-805AT). The carotid artery was examined with the head tilted slightly upward in the mid-line position. The transducer was manipulated so that the near and far walls were parallel to the transducer footprint, and the lumen diameter was maximized in the longitudinal plane.

According to the criteria of the European carotid plaque study group, plaques were classified into three different types: echolucent, intermediate and echo-rich plaques [12]. The visual classification of plaque echogenicity was independently performed by two sonographers with at least 5 years of experience in vascular imaging, and a kappa value (κ) was calculated to evaluate the between-observer agreement.

D. Image normalization

The ultrasound system settings (e.g. system gain, time gain compensation etc.) can impact the brightness and contrast of the B-mode images. In this study, all images were normalized according to the scheme proposed by Sabetai et al [24]. After normalization, the GSM of the blood range from 0 to 5, whereas the GSM of adventitia range from 185 to 195.

E. Statistics of the pixels in gray-level images of plaques

In this study, the plaque was manually segmented by one operator in the gray-level image, and the statistics of the pixels of plaques were obtained. Then, the AUCPDC analysis and GSM analysis were performed for each plaque based on their pixel statistics.

F. Gray-scale median

Here, we let x represents the gray scale pixel value, $f(x)$ is the probability density function of x , and $f(x)$ can be calculated as follows:

$$f(x) = \frac{\text{The number of pixels (gray value} = x)}{\text{Total number of pixels (gray value range from 0 to 255)}}. \quad (1)$$

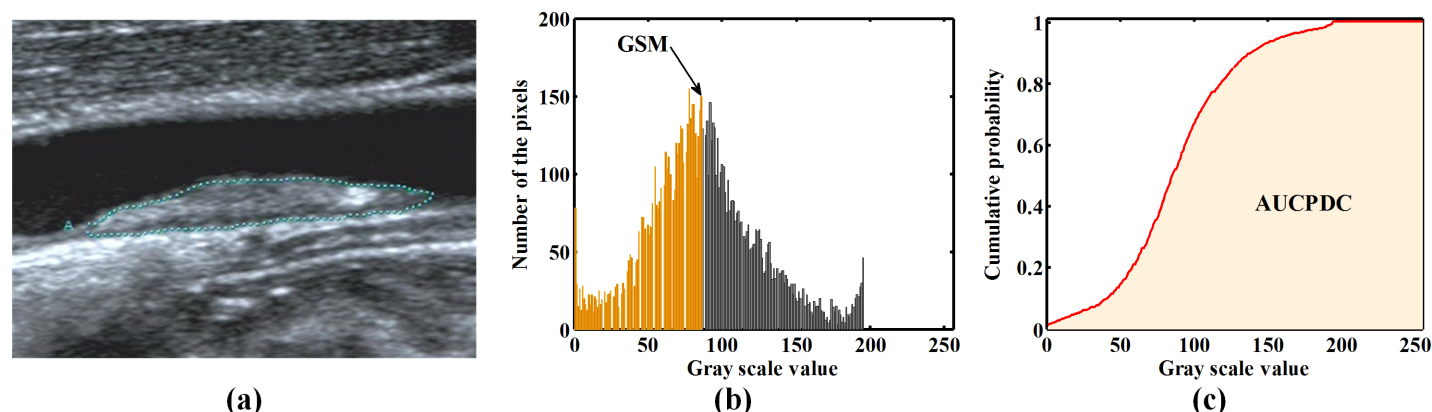


Fig 1. The GSM and AUCPDC of representative image of plaque. (a) Representative image of plaque; (b) When the orange area is 0.5, the horizontal coordinate value is GSM of the plaque illustrated in (a); (c) the shaded areas are the AUCPDC of the plaque illustrated in (a). Note that GSM = gray-scale median; AUCPDC = area under cumulative probability distribution curve.

<https://doi.org/10.1371/journal.pone.0185261.g001>

The GSM is defined as follows:

$$0.5 = \sum_{x=0}^{\text{GSM}} f(x) \quad (2)$$

where $f(x)$ is defined in Eq (1). A direct expression of GSM is shown in Fig 1B.

G. Area under cumulative probability distribution curve

For each plaque, the cumulative distribution function $F(x)$ of the gray scale distribution, can be expressed as follows,

$$F(x_i) = \sum_{x=0}^{x_i} f(x) \quad x = 0, 1, 2, \dots, 254, 255. \quad (3)$$

The AUCPDC is measured as follows,

$$\text{AUCPDC} = \sum_{x=0}^{255} F(x). \quad (4)$$

Fig 1C illustrates the AUCPDC (shaded area).

H. Classification

The k-nearest-neighbor (KNN) classification was performed for classifying the three different types of plaques based on AUCPDC or GSM. In order to improve the reliability of classification, a leave-one-out cross validation was implemented in this study. The kappa statistic (κ) was calculated to evaluate the agreement between visual classification and the KNN classification. Furthermore, the receiver operating characteristic (ROC) curves for the KNN classifier were developed to compare the ability of AUCPDC and GSM in identifying echolucent plaques.

I. Intra-operator agreement

In order to examine the intra-operator agreement, the AUCPDC analyses were performed at two different times within a 2-month period. Based on the same visual classification, a total of

45 plaques (15 echolucent, 15 intermediate and 15 echo-rich plaques) were randomly selected from the same original images, and the manual plaque segmentation was carried out again by the same operator. The intra-operator agreement was evaluated according to the method proposed by Bland and Altman [25].

J. Bootstrapping for estimating Youden's index J

Youden's index J [26] is a single statistic that can summarize the performance of a diagnostic test, and it is defined as:

$$J = \text{sensitivity} + \text{specificity} - 1. \quad (5)$$

It has been widely utilized in many studies to evaluate the accuracy of diagnostic tests and the performance of risk assessment model [27,28].

Bootstrap is a useful tool to provide statistical inference to estimate the accuracy and the precision of any statistic through resampling with replacement from the original datasets [29,30]. In this study, the bootstrapping is implemented to estimate the 95% confidence intervals (CIs) of Youden's index J .

K. Statistical analyses

All statistical analysis was performed with PASW Statistics 18 and all values were presented as the mean value \pm SD, or real number of patients with the percentage in parentheses.

[Spearman's rank correlation](#) analysis was also implemented between the GSM, AUCPDC and the status of hypertension, diabetes, coronary heart disease (CHD). Youden's index J was calculated using MedCalc statistical software.

Results

A. Patient characteristics

The baseline characteristics of the study population are shown in [Table 1](#). Among a total of 72 patients (51 male, 70.1%; age, 69.7 ± 8.7 years), 46 (63.9%) patients had hypertension, 31 (43.1%) had diabetes and 27 (37.5%) had CHD.

B. Visual classification

The classification of the carotid plaques ($n = 130$) into three different types showed a good agreement between two experienced sonographers ([Table 2](#)). The between-observer reproducibility was 96.15% ($\kappa = 0.942$). A total of 5 controversial plaques were excluded, and the 125 consensual plaques were retained in the following analysis.

C. The area under cumulative probability distribution curve of plaque

[Fig 2](#) shows the AUCPDC analysis of representative echolucent, intermediate and echo-rich plaques. The AUCPDC of echolucent plaques were largest, followed by intermediate plaques and echo-rich plaques ([Fig 2D](#)). The AUCPDC showed a statistical significance among the echo-rich, intermediate, echolucent plaques (130 ± 22 vs. 177 ± 18 vs. 207 ± 21 , $p < 0.001$). When type 1 denoted echo-rich, type 2 intermediate type 3 echolucent, the mean AUCPDC had a correlation with the types of plaques (Spearman $r = -0.856$, $p < 0.001$).

Table 1. Baseline characteristics of 72 patients.

Characteristics	Total (n = 72)
Age, mean (SD)	69.7 ± 8.7
Male gender, n (%)	51 (70.1)
Hypertension, n (%)	46 (63.9)
Smoking, n (%)	29 (40.3)
Diabetes, n (%)	31 (43.1)
CHD, n (%)	27 (37.5)
SBP (mm Hg)	136.5 ± 22.9
DBP (mm Hg)	77.0 ± 12.5
BMI (kg/m ²)	22.2 ± 2.7
TC (mmol/L)	4.26 ± 1.12
TG (mmol/L)	1.43 ± 1.14
HDL-C (mmol/L)	1.04 ± 0.27
LDL-C (mmol/L)	2.66 ± 0.95
ApoA1 (g/L)	1.19 ± 0.29
ApoB100 (g/L)	1.06 ± 0.38
FBG (mmol/L)	6.65 ± 2.87
HbA _{1c} (%)	6.31 ± 1.84

CHD = coronary heart disease; SBP = systolic blood pressure; DBP = diastolic blood pressure; BMI = body mass index; TC = total cholesterol; TG = triglycerides; HDL-C = high-density lipoprotein cholesterol; LDL-C = low-density lipoprotein cholesterol; ApoA1 = Apolipoprotein A1; ApoB100 = Apolipoprotein B100; FBG = fasting blood glucose.

<https://doi.org/10.1371/journal.pone.0185261.t001>

D. Carotid plaque classification

As shown in Tables 3 and 4, when AUCPDC was used for training classifier, the classification accuracy of discriminating the echo-rich, intermediate and echolucent plaques was 78.4% ($\kappa = 0.673$), which was higher than that obtained by using GSM 64.8% ($\kappa = 0.460$). When classification based on GSM, 8 of 35 intermediate plaques were classified correctly, and 21 of 35 intermediate plaques were misclassified as echolucent plaques (Table 3). The AUCPDC was more effective in discriminating intermediate and echolucent plaques than GSM. Table 4 indicated that 21 of 35 intermediate plaques were classified correctly, and 11 of 35 intermediate plaques were misclassified as echolucent plaques, when classification based on AUCPDC. Further, ROC curve analysis was developed to test the effectiveness of AUCPDC in the identification of echolucent plaques. The area under the curve (AUC) was 0.817 when AUCPDC was used for training the classifier, whereas AUC was 0.746 when GSM was used (Fig 3).

Table 2. Visual classification of 130 carotid plaques by two experienced sonographers.

		Sonographer 2			Total
		Echolucent	Intermediate	Echo-rich	
Sonographer 1	Echolucent	47	0	0	47
	Intermediate	3	35	0	38
	Echo-rich	1	1	43	45
	Total	51	36	43	130

$\kappa = 0.942$.

<https://doi.org/10.1371/journal.pone.0185261.t002>

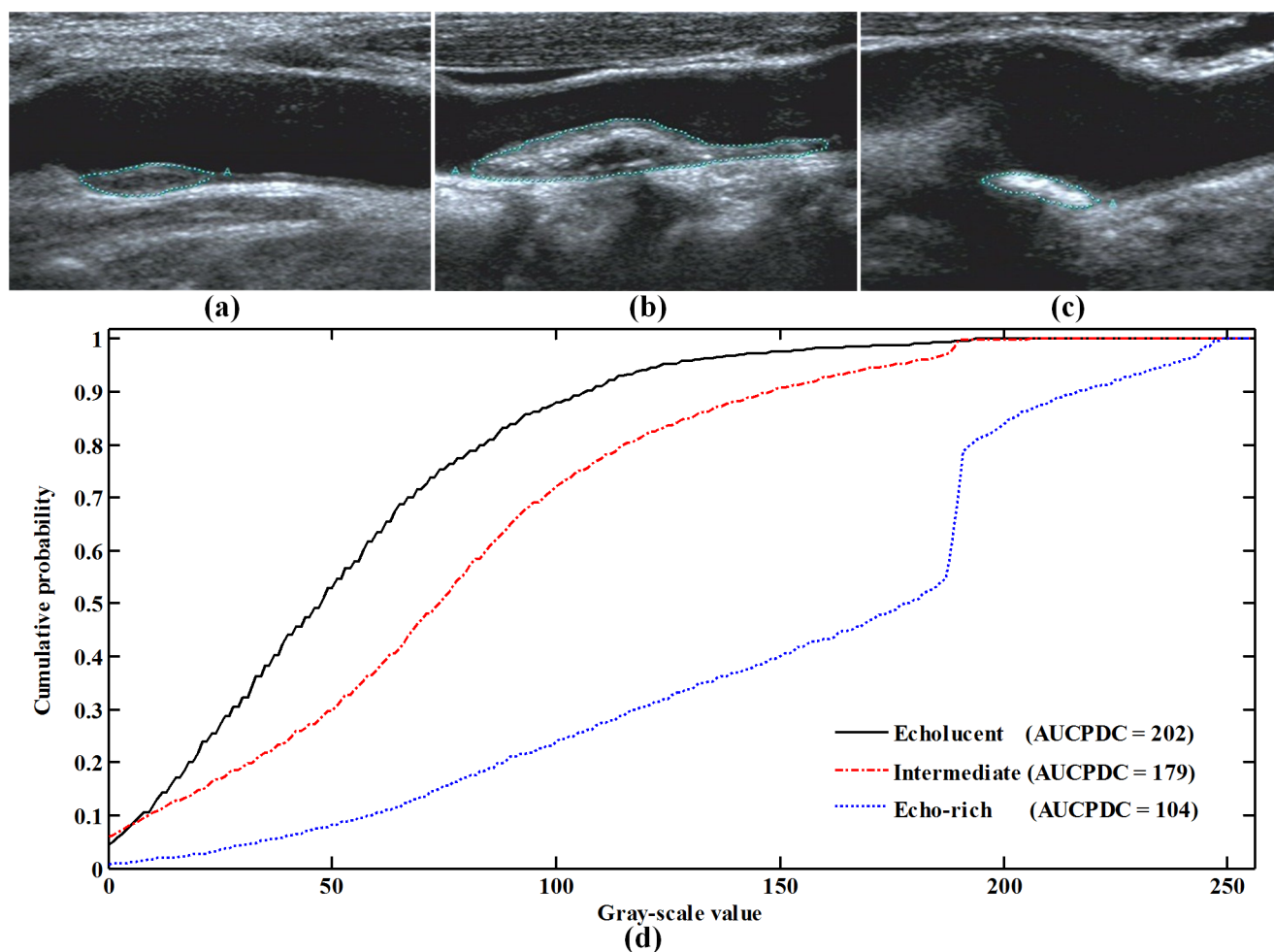


Fig 2. The AUCPDC of representative echolucent, intermediate and echo-rich plaques. The echolucent, intermediate and echo-rich plaques in (d) were defined in the original images (a), (b) and (c), respectively. Note that AUCPDC = area under cumulative probability distribution curve.

<https://doi.org/10.1371/journal.pone.0185261.g002>

E. Intra-operator agreement

Fig 4 illustrates the scatterplot of the average AUCPDC against the AUCPDC difference for 45 plaques that are analyzed at two different times within a 2-month period by one operator. Of the 45 points, there were 41 scattered in the Mean \pm 1.96 SD region (95% confidence level). The AUCPDC analysis showed a good intra-operator agreement.

F. Relationship between GSM, AUCPDC and hypertension, diabetes, CHD

Spearman's rank correlation analysis was implemented to examine the relationship between the GSM, AUCPDC and the status of hypertension, diabetes, CHD (Table 5). Compared with GSM, the AUCPDC showed a statistical association with CHD (Spearman $r = -0.121$, $p = 0.315$ vs. $r = 0.234$, $p = 0.050$).

G. Estimating Youden's index J in bootstrapping samples

When bootstrap was performed to estimate the Youden's index J , a total of 2000 bootstrapping samples was generated. The Youden's index J was 0.633 (95% CI: 0.479–0.753) when AUCPDC

Table 3. Classification of 125 carotid plaques based on GSM.

		GSM			Total
		Echolucent	Intermediate	Echo-rich	
Sonographers	Echolucent	37	8	2	47
	Intermediate	21	8	6	35
	Echo-rich	2	5	36	43
	Total	60	21	44	125

$\kappa = 0.460$.

<https://doi.org/10.1371/journal.pone.0185261.t003>

was used to train the classifier, whereas Youden's index J was 0.492 (95% CI: 0.326–0.633) when GSM was used.

Discussion

In the present study, the AUCPDC was proposed to evaluate plaque echogenicity. Our results indicated that it is feasible to classify echo-rich, intermediate and echolucent plaques based on AUCPDC. The classification accuracy was 78.4% ($\kappa = 0.673$), when AUCPDC was used to train the classifier. Previous studies have proven that the echolucent plaque is a high risk indicator of cardiovascular events [8,10,18,31,32]. Compared with GSM, the AUCPDC showed a higher potential feasibility for identifying echolucent plaques (AUC = 0.817) (Fig 3), and it was more related to CHD (Spearman $r = 0.234$, $p = 0.050$) (Table 5). These indicate that AUCPDC analysis of the ultrasound images of carotid plaques might have potential in predicting the cardiovascular risk in patients with plaques.

Many studies have shown that visual classification is a feasible and reliable method for classification of ultrasound plaques with different echogenicity [12,13,33]. Geroulakos et al. classified 70 carotid plaques into five different types (type 1 uniformly echolucent, type 2 predominantly echolucent, type 3 predominantly echogenic, type 4, uniformly echogenic, and type 5 calcified plaques) and the between-observer reproducibility was 85.71% ($\kappa = 0.79$). Mayor et al. analyzed 95 carotid bifurcation plaques with the same five-type classification system, and a between-observer reproducibility of 91% ($\kappa = 0.87$) was observed. In this study, the plaques were classified into three different types (type 1 echo-rich, type 2 intermediate and type 3 echolucent) according to the scheme of the European carotid plaque study group [12], and a higher between-observer reproducibility of 96.15% ($\kappa = 0.942$) was achieved.

Both GSM and AUCPDC are calculated based on the gray scale distribution. Compared with GSM, the AUCPDC calculation takes into consideration the probability density distribution of gray scale values ranging from 0 to 255. The lower gray scale value with a high probability density gives rise to a higher value of AUCPDC. Fig 5 illustrates that the sample 1 has a

Table 4. Classification of 125 carotid plaques based on AUCPDC.

		AUCPDC			Total
		Echolucent	Intermediate	Echo-rich	
Sonographers	Echolucent	37	10	0	47
	Intermediate	11	21	3	35
	Echo-rich	1	2	40	43
	Total	49	33	43	125

$\kappa = 0.673$.

<https://doi.org/10.1371/journal.pone.0185261.t004>

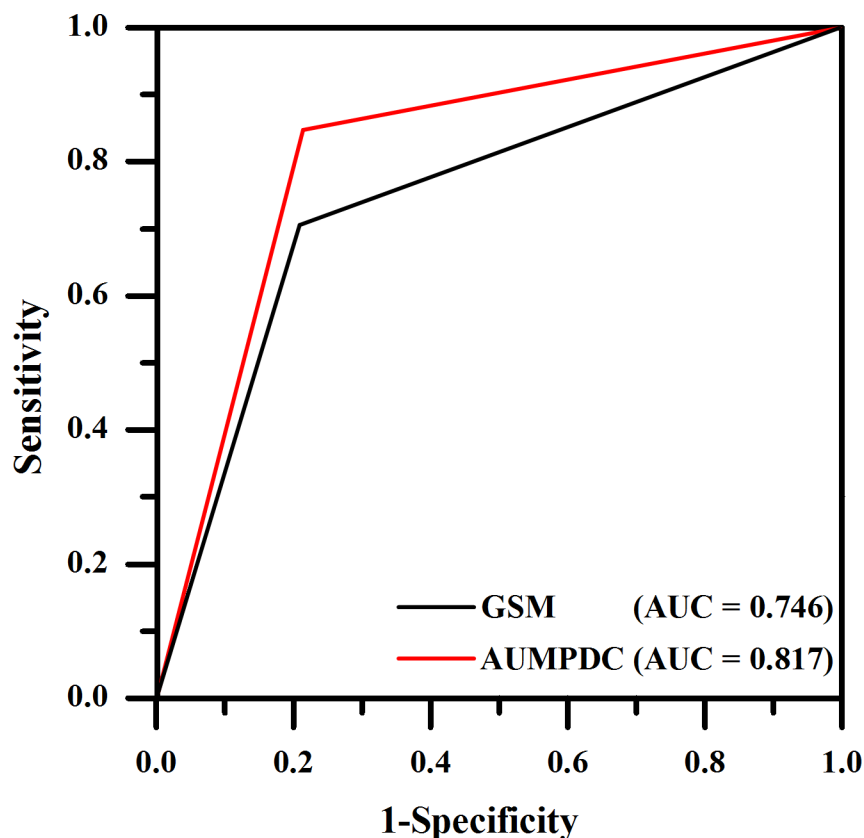


Fig 3. Receiver operating characteristic curves of identifying echolucent plaques for KNN classifier using AUCPDC and GSM. Note that AUC = area under the curve; GSM = gray-scale median; AUCPDC = area under cumulative probability distribution curve.

<https://doi.org/10.1371/journal.pone.0185261.g003>

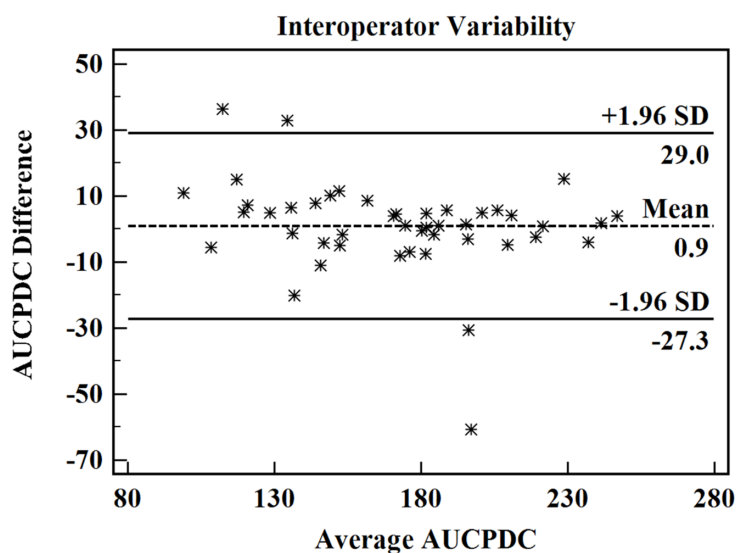


Fig 4. Scatterplot of the average AUCPDC against the AUCPDC difference for 45 plaques analyzed at 2 different times within a 2-month period by one operator. Note that AUCPDC = area under cumulative probability distribution curve.

<https://doi.org/10.1371/journal.pone.0185261.g004>

Table 5. Spearman's rank correlation between the GSM, AUCPDC and the status of hypertension, diabetes, CHD.

		Hypertension	Diabetes	CHD
GSM	Spearman r	-0.031	-0.071	-0.121
	p	0.798	0.554	0.315
AUCPDC	Spearman r	0.1	-0.035	.234
	p	0.402	0.770	0.050*

GSM = gray-scale median; AUCPDC = area under cumulative probability distribution curve, CHD = coronary heart disease.

<https://doi.org/10.1371/journal.pone.0185261.t005>

same GSM with sample 2 (GSM = 128), but the AUCPDC of sample 2 is larger than sample 1. It may imply that AUCPDC is more effective than GSM in distinguishing the differences in the probability density distributions of gray scale value of plaques. Consistent with the above analysis, Tables 3 and 4 indicate that AUCPDC shows an obvious superiority in discriminating intermediate and echolucent plaques.

In this research, compared with GSM, the AUCPDC showed a statistical association with CHD ($p = 0.05$) (Table 5), but the correlation is barely significant. Such results may be caused by the relatively small sample size and sample difference. Among a total of 72 patients in this study, only 27 (37.5%) patients had CHD. What's more, there are some methodological limitations on the calculation of AUCPDC. The ultrasound system settings (e.g. system gain, time gain compensation etc.) impact the brightness and contrast of the B-mode images, which will cause calculation bias in AUCPDC. To reduce the impact of instrument settings, normalization of the dynamic range is done by considering minimum and maximum pixel intensities within the region-of-interest. Overall, the AUCPDC is an effective parameter for evaluating the plaque echogenicity.

Conclusion

Compared with GSM, the AUCPDC is more effective in classifying three types of plaques and identifying echolucent plaques, suggesting that AUCPDC analysis is a promising method for

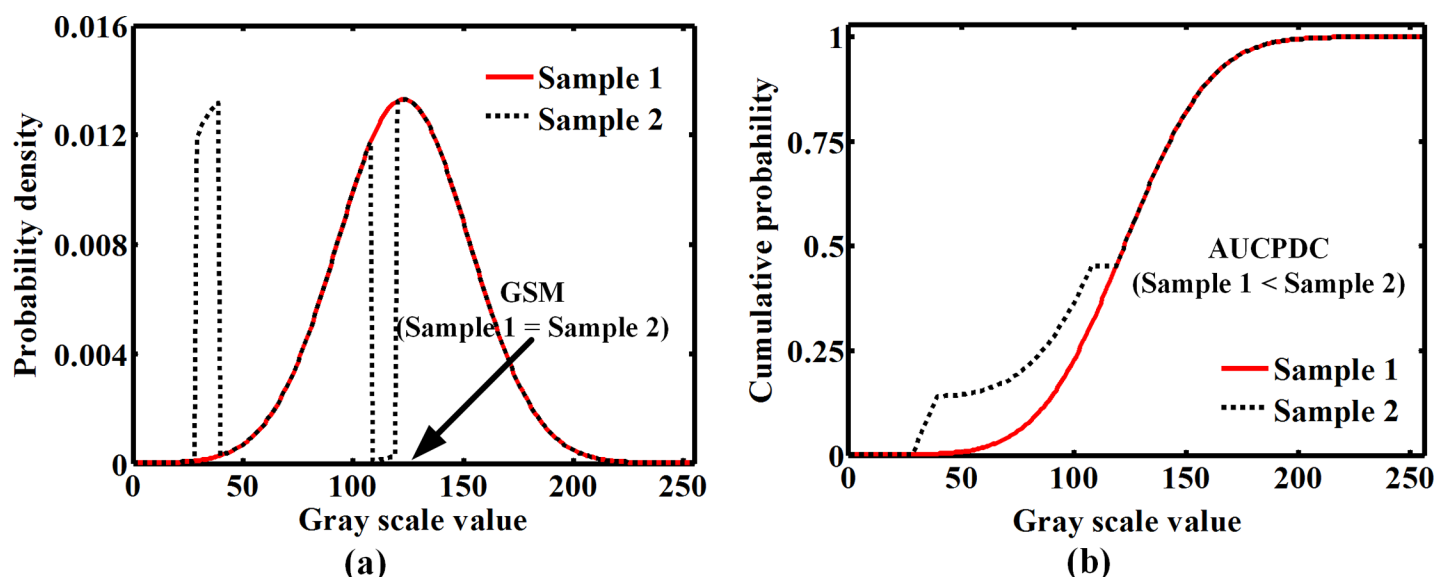


Fig 5. A comparison between AUCPDC with GSM when the probability density curve is changed. Note that GSM = gray-scale median; AUCPDC = area under cumulative probability distribution curve.

<https://doi.org/10.1371/journal.pone.0185261.g005>

evaluating plaque echogenicity and predicting cardiovascular risk in patients with plaques. However, this study is limited by the relatively small number of plaques, thus future research is required to further validate our results. Furthermore, a longitudinal, prospective study utilizing carotid ultrasound examination in a large number of patients with atherosclerotic risk is required to assess the value of AUCPDC in predicting the future cardiovascular events.

Supporting information

S1 Supporting Information. Baseline characteristics.
(XLSX)

S2 Supporting Information. Matlab code. Classification base on a leave-one-out strategy.
(M)

Author Contributions

Conceptualization: Xiaowei Huang, Ming Qian, Hairong Zheng, Lili Niu.

Data curation: Xiaowei Huang, Yanling Zhang, Long Meng, Derek Abbott, Rongqing Zheng.

Funding acquisition: Hairong Zheng, Lili Niu.

Methodology: Xiaowei Huang, Yanling Zhang, Ming Qian.

Project administration: Hairong Zheng.

Resources: Yanling Zhang, Rongqing Zheng.

Software: Xiaowei Huang, Ming Qian.

Supervision: Ming Qian, Kelvin K. L. Wong, Rongqing Zheng, Hairong Zheng, Lili Niu.

Validation: Yanling Zhang, Kelvin K. L. Wong, Lili Niu.

Visualization: Xiaowei Huang, Long Meng, Ming Qian, Lili Niu.

Writing – original draft: Xiaowei Huang, Long Meng, Derek Abbott, Kelvin K. L. Wong, Hairong Zheng, Lili Niu.

Writing – review & editing: Xiaowei Huang, Long Meng, Derek Abbott, Hairong Zheng, Lili Niu.

References

1. Yusuf S, Reddy S, Ounpuu S, Anand S (2001) Global burden of cardiovascular diseases: part I: general considerations, the epidemiologic transition, risk factors, and impact of urbanization. *Circulation* 104: 2746–2753. PMID: [11723030](https://pubmed.ncbi.nlm.nih.gov/11723030/)
2. Mozaffarian D, Benjamin EJ, Go AS, Arnett DK, Blaha MJ, Cushman M, et al. (2015) Heart disease and stroke statistics—2015 update: a report from the American Heart Association. *Circulation* 131: e29–322. <https://doi.org/10.1161/CIR.000000000000152> PMID: [25520374](https://pubmed.ncbi.nlm.nih.gov/25520374/)
3. Mathiesen EB, Bonna KH, Joakimsen O (2001) Echolucent plaques are associated with high risk of ischemic cerebrovascular events in carotid stenosis: The Tromso study. *Circulation* 103: 2171–2175. PMID: [11331258](https://pubmed.ncbi.nlm.nih.gov/11331258/)
4. Ruiz-Ares G, Fuentes B, Martinez-Sanchez P, Diez-Tejedor E (2014) A prediction model for unstable carotid atheromatous plaque in acute ischemic stroke patients: proposal and internal validation. *Ultrasound Med Biol* 40: 1958–1965. <https://doi.org/10.1016/j.ultrasmedbio.2014.04.015> PMID: [25023112](https://pubmed.ncbi.nlm.nih.gov/25023112/)
5. Nordestgaard BG, Gronholdt ML, Silleisen H (2003) Echolucent rupture-prone plaques. *Curr Opin Lipidol* 14: 505–512. <https://doi.org/10.1097/01.mol.0000092628.86399.9f> PMID: [14501590](https://pubmed.ncbi.nlm.nih.gov/14501590/)

6. Gronholdt ML, Wiebe BM, Laursen H, Nielsen TG, Schroeder TV, Sillesen H (1997) Lipid-rich carotid artery plaques appear echolucent on ultrasound B-mode images and may be associated with intraplaque haemorrhage. *Eur J Vasc Endovasc Surg* 14: 439–445. PMID: [9467517](#)
7. Roy J, Hedin U (2016) Commentary on 'plaque echolucency and the risk of ischaemic stroke in patients with asymptomatic carotid stenosis within the first asymptomatic carotid surgery trial (ACST-1)'. *Eur J Vasc Endovasc Surg* 51: 622. <https://doi.org/10.1016/j.ejvs.2016.01.002> PMID: [26919935](#)
8. Honda O, Sugiyama S, Kugiyama K, Fukushima H, Nakamura S, Koide S, et al. (2004) Echolucent carotid plaques predict future coronary events in patients with coronary artery disease. *J Am Coll Cardiol* 43: 1177–1184. <https://doi.org/10.1016/j.jacc.2003.09.063> PMID: [15063426](#)
9. Hirano M, Nakamura T, Kitta Y, Sano K, Kodama Y, Kobayashi T, et al. (2010) Assessment of carotid plaque echolucency in addition to plaque size increases the predictive value of carotid ultrasound for coronary events in patients with coronary artery disease and mild carotid atherosclerosis. *Atherosclerosis* 211: 451–455. <https://doi.org/10.1016/j.atherosclerosis.2010.03.003> PMID: [20362290](#)
10. Nakamura T, Kitta Y, Uematsu M, Sugamata W, Hirano M, Fujioka D, et al. (2013) Ultrasound assessment of brachial endothelial vasomotor function in addition to carotid plaque echolucency for predicting cardiovascular events in patients with coronary artery disease. *Int J Cardiol* 167: 555–560. <https://doi.org/10.1016/j.ijcard.2012.01.064> PMID: [22326513](#)
11. Doonan RJ, Dawson AJ, Kyriacou E, Nicolaides AN, Corriveau MM, Steinmetz OK, et al. (2013) Association of ultrasonic texture and echodensity features between sides in patients with bilateral carotid atherosclerosis. *Eur J Vasc Endovasc Surg* 46: 299–305. <https://doi.org/10.1016/j.ejvs.2013.05.024> PMID: [23849798](#)
12. European Carotid Plaque Study Group (2011) Reprinted article "Carotid artery plaque composition—relationship to clinical presentation and ultrasound B-mode imaging". *Eur J Vasc Endovasc Surg* 42 Suppl 1: S32–S38.
13. Mayor I, Momjian S, Lalive P, Sztajzel R (2003) Carotid plaque: comparison between visual and grey-scale median analysis. *Ultrasound Med Biol* 29: 961–966. PMID: [12878241](#)
14. Pahl U, Holdfeldt P, Bergstrom G, Fagerberg B, Hulthe J, Gustavsson T (2010) Percentage white: a new feature for ultrasound classification of plaque echogenicity in carotid artery atherosclerosis. *Ultrasound Med Biol* 36: 218–226. <https://doi.org/10.1016/j.ultrasmedbio.2009.10.002> PMID: [20018430](#)
15. Christodoulou CI, Pattichis CS, Pantziaris M, Nicolaides A (2003) Texture-based classification of atherosclerotic carotid plaques. *IEEE Trans Med Imaging* 22: 902–912. <https://doi.org/10.1109/TMI.2003.815066> PMID: [12906244](#)
16. Tsiaparas NN, Golemati S, Andreadis I, Stoitsis JS, Valavanis I, Nikita KS (2011) Comparison of multi-resolution features for texture classification of carotid atherosclerosis from B-mode ultrasound. *IEEE Trans Inf Technol Biomed* 15: 130–137. <https://doi.org/10.1109/TITB.2010.2091511> PMID: [21075733](#)
17. Acharya UR, Sree SV, Krishnan MM, Molinari F, Saba L, Ho SY, et al. (2012) Atherosclerotic risk stratification strategy for carotid arteries using texture-based features. *Ultrasound Med Biol* 38: 899–915. <https://doi.org/10.1016/j.ultrasmedbio.2012.01.015> PMID: [22502883](#)
18. Irie Y, Katakami N, Kaneto H, Takahara M, Nishio M, Kasami R, et al. (2013) The utility of ultrasonic tissue characterization of carotid plaque in the prediction of cardiovascular events in diabetic patients. *Atherosclerosis* 230: 399–405. <https://doi.org/10.1016/j.atherosclerosis.2013.08.015> PMID: [24075774](#)
19. Salem MK, Bown MJ, Sayers RD, West K, Moore D, Nicolaides A, et al. (2014) Identification of patients with a histologically unstable carotid plaque using ultrasonic plaque image analysis. *Eur J Vasc Endovasc Surg* 48: 118–125. <https://doi.org/10.1016/j.ejvs.2014.05.015> PMID: [24947079](#)
20. Huang X, Zhang Y, Qian M, Meng L, Xiao Y, Niu L, et al. (2016) Classification of carotid plaque echogenicity by combining texture features and morphologic characteristics. *J Ultrasound Med* 35: 2253–2261. <https://doi.org/10.7863/ultra.15.09002> PMID: [27582533](#)
21. Shankar PM, Forsberg F, Lown L (2003) Statistical modeling of atherosclerotic plaque in carotid B mode images—a feasibility study. *Ultrasound Med Biol* 29: 1305–1309. PMID: [14553808](#)
22. Expert Committee on the Diagnosis and Classification of Diabetes Mellitus (2003) Report of the expert committee on the diagnosis and classification of diabetes mellitus. *Diabetes Care* 26 Suppl 1: S5–20.
23. Goldenberg R, Punthakee Z (2013) Definition, classification and diagnosis of diabetes, prediabetes and metabolic syndrome. *Can J Diabetes* 37 Suppl 1: S8–11.
24. Sabetai MM, Tegos TJ, Nicolaides AN, Dhanjil S, Pare GJ, Stevens JM (2000) Reproducibility of computer-quantified carotid plaque echogenicity: Can we overcome the subjectivity? *Stroke* 31: 2189–2196. PMID: [10978050](#)
25. Bland JM, Altman DG (1986) Statistical methods for assessing agreement between two methods of clinical measurement. *Lancet* 1: 307–310. PMID: [2868172](#)
26. Youden WJ (1950) Index for rating diagnostic tests. *Cancer* 3: 32–35. PMID: [15405679](#)

27. Heider P, Pfaffle N, Pelisek J, Wildgruber M, Poppert H, Rudelius M, et al. (2010) Is serum pregnancy-associated plasma protein a really a potential marker of atherosclerotic carotid plaque stability? *Eur J Vasc Endovasc Surg* 39: 668–675. <https://doi.org/10.1016/j.ejvs.2010.03.012> PMID: [20399126](#)
28. Giede-Jeppe A, Bobinger T, Gerner ST, Madzar D, Sembill J, Lucking H, et al. (2016) Lymphocytopenia is an independent predictor of unfavorable functional outcome in spontaneous intracerebral hemorrhage. *Stroke* 47: 1239–1246. <https://doi.org/10.1161/STROKEAHA.116.013003> PMID: [27073240](#)
29. Efron B (1992) *Bootstrap methods: another look at the jackknife*. Breakthroughs in statistics: Springer. pp. 569–593.
30. Efron B, Tibshirani RJ (1994) *An introduction to the bootstrap*: CRC press.
31. Gronholdt ML, Nordestgaard BG, Schroeder TV, Vorstrup S, Sillesen H (2001) Ultrasonic echolucent carotid plaques predict future strokes. *Circulation* 104: 68–73. PMID: [11435340](#)
32. Reiter M, Effenberger I, Sabeti S, Mlekusch W, Schlager O, Dick P, et al. (2008) Increasing carotid plaque echolucency is predictive of cardiovascular events in high-risk patients. *Radiology* 248: 1050–1055. <https://doi.org/10.1148/radiol.2483071817> PMID: [18710994](#)
33. Geroulakos G, Ramaswami G, Nicolaides A, James K, Labropoulos N, Belcaro G, et al. (1993) Characterization of symptomatic and asymptomatic carotid plaques using high-resolution real-time ultrasonography. *Br J Surg* 80: 1274–1277. PMID: [8242296](#)